ELECTROMECHANICAL CHARACTERISTICS OF POLYVINYLIDENE FLUORIDE FOR FLEXIBLE ELECTRONICS

Wen-Yang Chang and Cheng-Hung Hsu
Department of Mechanical and Computer-Aided Engineering,
National Formosa University, Yunlin County, 632, Taiwan
E-mail: wenyang@nfu.edu.tw

ICETI 2012-A1022_SCI
No. 13-CSME-19, E.I.C. Accession 3477

ABSTRACT

The electromechanical characteristics of PVDF are investigated, including the crystallization, frequency responses, hysteresis, leakage currents, current-voltage characteristics, and fatigue characteristics using X-ray diffraction and an electrometer. Results show that the frequency band of PVDF increases with increasing resistive load and capacitance. The hysteresis area of ΔH slightly increases with increasing input voltage. The magnitude of the current values increases with decreasing delay time at a given drive voltage. PVDF film induced larger degradation when the number of stress cycles was increased to about 10^5 cumulative cycles.

Keywords: PVDF; electromechanical; leakage current; fatigue; frequency response.

CARACTÉRISTIQUES ÉLECTROMÉCANIQUES DU POLYFLUORE DE VINYLIDÈNE POUR CIRCUITS IMPRIMÉS SOUPLES

RÉSUMÉ

Les caractéristiques électromécaniques du polyfluore de vinylidène (PVDF) font l'objet de cette étude, incluant la cristallisation, la réponse en fréquence, l'hystérésis, le courant de fuite, les caractéristiques dipôles électriques, et les caractéristiques de fatigue mesurées par diffraction de rayons X et un électromètre. Les résultats indiquent que la bande de fréquence du film PVDF augmente avec l'accroissement de la charge résistive et la capacitance. La zone d'hystérésis de ΔH est légèrement accrue avec une augmentation de la tension d'entrée. La magnitude des valeurs actuelles augmente avec un délai d'attente décroissant pendant une tension de commande donnée. Le film PVDF a induit une dégradation plus grande quand le nombre de cycles de contraintes a été augmenté à près de 10^5 cycles cumulatifs.

Mots-clés : polyfluore de vinylidène (PVDF) ; électromécanique ; courant de fuite ; fatigue ; réponse en fréquence.

NOMENCLATURE

A	active area
C	capacitance
E	applied electric filed
e	scaling electric field
f	break frequency
n	average density
p	applied pressure
P_S	saturation polarization
P_A	anhysteretic polarization
R	resistive load
T	operating temperature
T_c	Curie temperature
t	thickness
ε_r	relative permittivity
ε_o	permittivity of free space
ε_s	surface energy of the domain wall
ε	effective field energy
ω	natural frequency

1. INTRODUCTION

Polyvinylidene fluoride (PVDF) combined with piezoelectricity or pyroelectricity has become attractive for application in flexible electronics [1, 2]. Mechanical vibration by a piezoelectric material is used in numerous applications [3, 4]. Materials used for piezoelectric energy harvesting include zirconium titanate (PZT), aluminum nitride (AlN), barium titanate (BaTi03), and zinc oxide (ZnO) [5–7]. Generally speaking, crystal and ceramic piezoelectric materials in bulk and film forms are not suitable for flexible substrates due to their high required annealing temperatures. To harvest piezoelectric energy using flexible materials, the piezoelectric materials must be obtained using low-temperature fabrication and have sufficient flexibility to be implemented on a flexible substrate [8].

Low-power generators based on flexible electronics can be applied to wireless devices, such as radio-frequency identification (RFID) and micro-actuators for self-energy harvesting [9]. Solar energy, thermal energy, and mechanical vibrations can be harvested for generating energy. However, solar cells have limited use in low-light conditions and thermal energy is a low transduction into electrical energy due to power consumption. Mechanical vibration from a piezoelectric material is used in numerous applications. PVDF is beginning to be applied in flexible electronics due to its good mechanical strength, electrochemical stability, flexibility, and its ability to be cut apart freely [10]. Investigating the characteristics of PVDF for flexible applications is thus important. Although the phase transformations at various stretching ratios [11, 12], the thermomechanical characteristics [13, 14], and the mechanical characteristics [15, 16] of PVDF have been widely investigated, few studies have focused on its electromechanical properties and long duration analysis [17]. Therefore, this study investigates the frequency response, hysteresis, leakage currents, current-voltage (I-V) characteristics, and the fatigue characteristics of PVDF films.

2. EXPERIMENT

2.1. PVDF Films

PVDF films (Measurement Specialties Inc.) with a density of 1.78 g/ml, a piezo strain constant of $d_{31} = 23 \times 10^{-12}$ C/N, and a piezo stress constant of $g_{31} = 23 \times 10^{-12}$ C/N were used.

PVDF samples were cut into a rectangular shape with a thickness of 28 μm. Silver ink electrodes with an active sensing area of approximately 12×30 mm were used. The equivalent circuit of PVDF film comprises an AC voltage source and a capacitor connected in series. The AC voltage source represents the piezoelectric generator, whose voltage is produced by applied pressure. The capacitance is expressed as

$$C = \varepsilon_r \varepsilon_0 \frac{A}{t}, \qquad (1)$$

where ε_r and ε_0 are the relative permittivity and the permittivity of free space (8.854×10^{-12} F/m), respectively. A and t are the active area and thickness of PVDF film, respectively.

2.2. Characteristic Analysis

The PVDF films were characterized using X-ray diffraction (XRD, D8-DISCOVER, Bruker, USA). XRD was used to identify the crystalline structures of PVDF films. During XRD measurements, the step scanning was performed at 0.05° intervals and a radiation λ of 1.54Å was used as the X-ray source.

The electromechanical characteristics of the PVDF film were measured using an electrometer (RT66B, Radiant Technologies Inc., USA). The electrical response is capable of executing a single-pass hysteresis loop in 5 ms and the minimum leakage resolution is about 10 pA. During the electrical measurements, the DRIVE channel in the instrument provided a stimulus voltage for the top electrode of the PVDF sample and the RETURN channel integrated the charge from the bottom electrode of PVDF sample, captured at 0 V. The parasitic capacitance between the DRIVE and RETURN was approximately 1 pF.

3. CONCLUSIONS & DISCUSSIONS

The effects of frequency response, hysteresis, leakage currents, I-V characteristics, and fatigue characteristics were measured. They are described in the following subsections.

3.1. Crystallization Characteristics

The PVDF crystallization was detected using XRD. PVDF film is a semi-crystallized polymer that has at least four possible crystalline structures, denoted as α, β, γ, and δ, respectively. PVDF film without ferroelectric characteristics consists of the α crystalline phase; the β phase is generally obtained by mechanical stretching; the γ phase is obtained by annealing the film at temperatures near the melting point; and the δ phase can be produced by electric poling. In general, the β form has the trans-trans-trans-trans (TTTT) conformation, which is called the planar-zigzag structure. XRD was used to identify the crystalline structures of PVDF films with α or β phases. The β phase is desirable due to its ferroelectric characteristics. Figure 1 shows the XRD pattern of PVDF. The PVDF films are mostly the β phase.

3.2. Frequency Responses

The PVDF frequency responses were obtained at various resistive loads and capacitances using OrCAD Pspice software. The dashed line in the inset of Fig. 2a represents the results obtained for the equivalent circuit of PVDF film. During the analysis, the frequency response was measured in the range of 1 Hz to 1 MHz using an AC sweep with a logarithmic scale. The range of resistive loads was 100 kΩ to 1 MΩ, measured in intervals of 100 kΩ. The values of the AC voltage source and the capacitance were assumed to be 1 Vac and 2.6 nF, respectively.

The frequency responses of the PVDF model for various resistive loads are shown in Fig. 2a. The resistive load forms a potential divider with RC characteristics. The results show that the PVDF model exhibits high-pass filter characteristics. The frequency band of the PVDF film increases with increasing resistive load. The break frequencies for 100, 300, 700 kΩ and 1 MΩ at the break frequency are 611, 207, 88, and 61 Hz, respectively. The output response is significantly reduced when the PVDF film is operated below the break

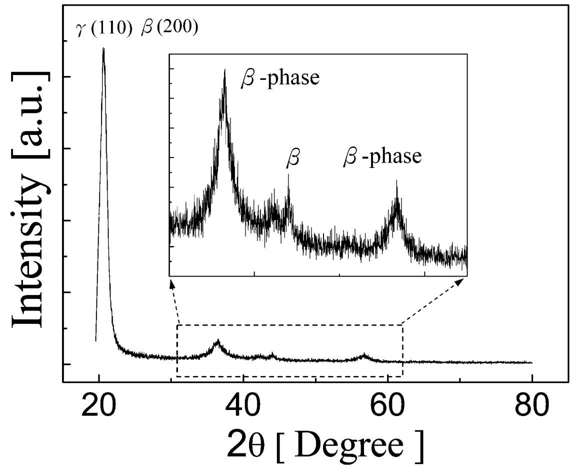

Fig. 1. XRD diffraction patterns of PVDF crystallization.

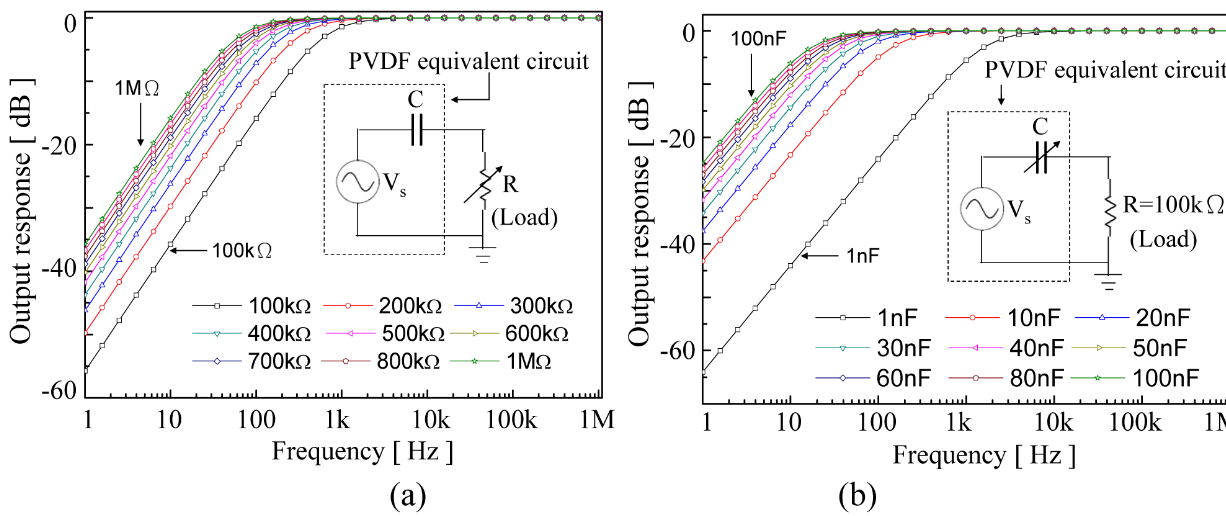

Fig. 2. Frequency responses of PVDF for various (a) resistive loads and (b) PVDF's capacitances.

frequency. For low-frequency measurements, the input resistance needs to be sufficiently high for the break frequency to be well below the designed operating frequency. The resistive load, R, can be evaluated as

$$R = 142.97 + 1838.23 \times e^{(1/75.77)f}, \tag{2}$$

where f is the break frequency. Figure 2b shows the frequency responses of PVDF film for various capacitances. In general, the capacitance is related to the area of PVDF film. The results show that the resistive load exhibits high-pass filter characteristics. The frequency band of PVDF film increases with increasing capacitance. The break frequencies for 1, 30, 60, and 100 nF at the break frequency are 1.585 kHz, 52.148, 31.875 and 17.712 Hz, respectively. The output response is significantly reduced when the PVDF film is operated below the break frequency. The capacitance, C, can be evaluated as

$$C = 1.0535 + 216.59 \times e^{(1/12.24)f} + 46.42 \times e^{(1/87.32)f}, \tag{3}$$

where f is the break frequency.

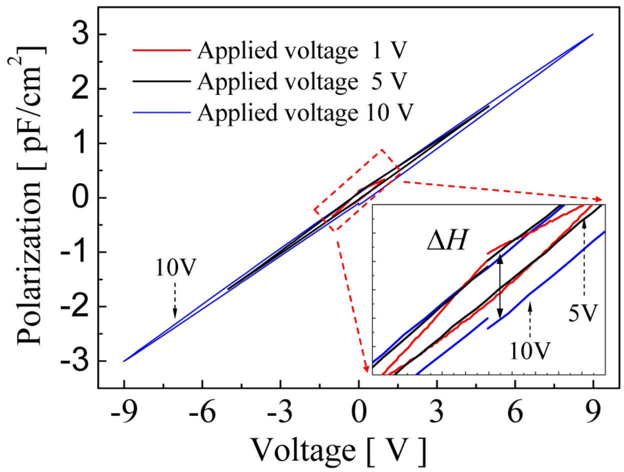

Fig. 3. Hysteresis characteristics of piezoelectric PVDF films for various applied voltages.

3.3. Hysteresis Characteristics

Piezoelectric PVDF material exhibits ferroelectric characteristics and has spontaneous polarization that can be reversed by applying an electric field. In general, the total polarization P is the sum of reversible polarization P_{rev} and irreversible polarization P_{ir} [18]:

$$P = P_{\text{ir}} + P_{\text{rev}} = \left(P_A - \frac{n\varepsilon}{2p}\frac{dP_{\text{ir}}}{dE}\right) + \frac{c}{1+c}(P_A - P_{\text{ir}}), \tag{4}$$

where

$$P_A = P_S \tanh\left(\frac{3ET_C}{eT}\right), \quad c = \frac{p\pi y^4 k_1}{4\varepsilon_s}, \quad \text{and} \quad P_{\text{ir}} = P_A - \frac{n\varepsilon}{2p}\frac{dP_{\text{ir}}}{dE}.$$

E, e, P_S, and P_A are the applied electric filed, the scaling electric field, the saturation polarization, and the anhysteretic polarization, respectively. T and T_c are the operating and Curie temperatures of PVDF, respectively. ε_s, ε, p, and n denote the surface energy of the domain wall, the effective field energy, the applied pressure, and the average density of pinning sites, respectively. The anhysteretic polarization represents the minimal energy states and dipole rotation toward preferred ionic configurations. It saturates at high field levels. The hysteresis is usually nonlinear and is difficult to control appropriately if it is not measured accurately.

Figure 3 shows the hysteresis characteristics of piezoelectric PVDF film for various applied voltages. The hysteresis area of ΔH slightly increases and polarization increases linearly with increasing input voltage. The maximum polarizations for applied voltages of 1, 5, and 10 V are 0.37, 1.531, and 3.07 pF/cm^2, respectively. The polarization decreases when the applied voltage decreases from the saturation point to a negative saturation point. The hysteretic behavior of PVDF is due to the loss nature of the piezoelectric material where the current trails the applied voltage by an angle α that is related to the loss tangent of the material. The loop form of ΔH hysteresis is attributed to the impediment of the domain wall movement and the stress non-homogeneities inherent to the domain structure of the material, indicated that the energy required to translate domain walls by defects in material due to the reduction in energy.

3.4. Leakage Currents

The equivalent circuit of PVDF film comprises a voltage source in series with a capacitance. The leakage current depends on the input voltage according to Ohm's Law. For PVDF leakage current measurements, the

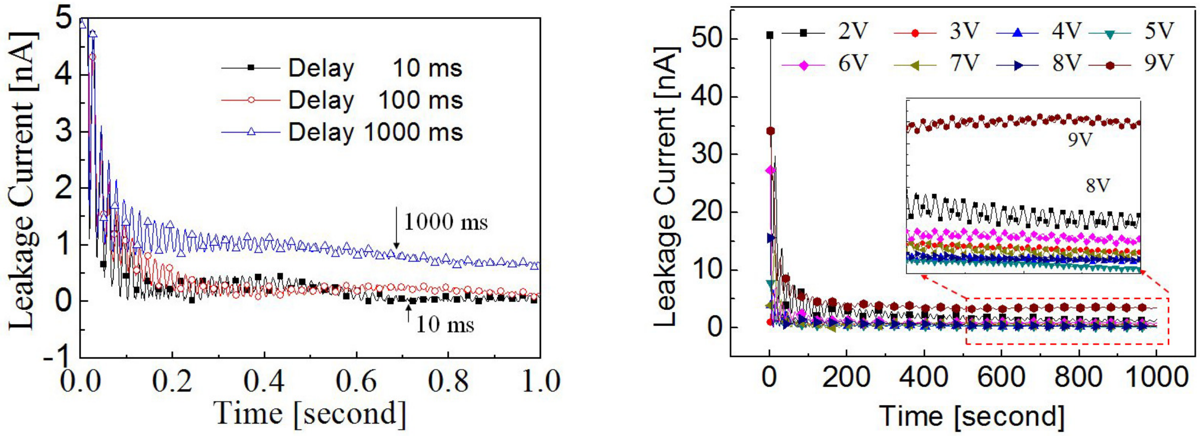

Fig. 4. Leakage currents of PVDF film at room temperature (a) with delay times of 10, 100, and 1000 ms at a voltage of 5 V and (b) with DC bias voltages of 2 to 9 V.

samples were subjected to a constant DC bias voltage. The steady-state current through the PVDF film was measured using a multimeter. The main parameters for the leakage measurement are the delay time, the DC bias voltage, and the measurement time. The delay time is the time it takes for the PVDF sample to reach a steady- state voltage. Therefore, PVDF sample is to allow the current induced by switching polarization to dampen and settle so that the sample is in steady-state current. After the delay time, the measurement period begins, during which current flows through the sample. The DC bias voltage produces an electric field for leakage current of conduction mechanism. The measurement time, step time, and step preset pulse voltage are 100 ms, 10 ms, and 9 V, respectively, at in switched linear mode.

Figure 4a shows leakage currents of the PVDF sample for delay times of 10, 100, and 1000 ms, respectively, obtained at a voltage of 5 V at room temperature. The characteristic responses initially have a large disturbance. The leakage current of PVDF film is higher for a lower delay time for a given applied electric field. The average leakage currents for delay times of 10, 100, and 1000 ms are 0.565, 19.9, and 73.8 pA, respectively. In general, the delay time is associated with irreversible thermodynamic change. The leakage currents of PVDF film with DC bias voltages of 2 to 9 V are shown in Fig. 4b. The leakage currents are similar when the DC bias voltage is under 7 V. The maximum leakage current (3.46 pA) was obtained for an input voltage of 9 V. The increase in leakage current is caused by electrically conductive channels spreading out within the PVDF due to material breakdown. In addition, temperature affects leakage current via piezoelectric coupling and electricmechanical losses.

3.5. Current-Voltage Characteristics

The I-V characteristics were measured in switched linear mode, where the preset pulse of the voltage is inverted to the measurement voltage. The preset pulse puts the sample into a polarization state, which ensures that the measurement will switch the PVDF film. Figure 5 shows the I-V characteristics of PVDF film for various delay times for voltages of −9 to 9 V. The magnitude of the current values increases with decreasing delay time for a given drive voltage. The increase in current is attributed to improved formation of charge transfer complexes. This allows the current from remanent or non-remanent polarization switching in the PVDF film to settle and reach a steady state. The PVDF film exhibits Schottky-like I-V characteristics. Similar and repeatable I-V characteristics were measured when the delay time was larger than about 2 ms.

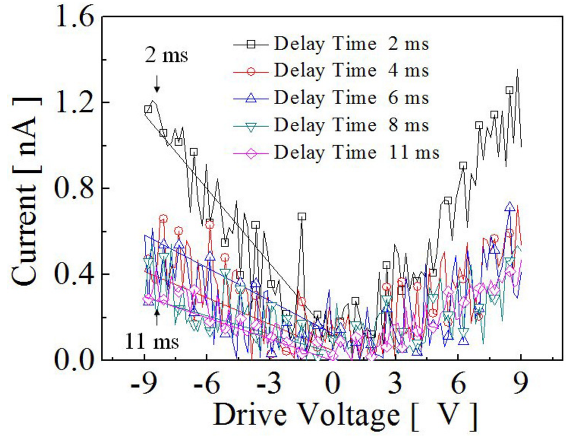

Fig. 5. Current-voltage characteristics of PVDF film for various delay times and voltages of −9 to 9 V.

The I-V characteristics of PVDF film can be described as [19]:

$$V = \frac{R}{\sqrt{1+(\omega RC)^2}} \times I, \tag{5}$$

where R, C, and ω are the impedance and the capacitance of the PVDF equivalent circuit, and the natural frequency, respectively. Therefore, the I-V characteristic response depends on these values.

3.6. Fatigue Characteristics

The fatigue characteristics were measured to determine the damage mechanism due to electrical stress of ferroelectric PVDF film undergoing repeated switching. Fatigue is a major issue for the reliability and reduplication of PVDF films since a loss of polarization can produce incorrect readings and limit lifetime. Fatigue is a function of stress voltage and frequency for polarization switching and non-switching polarization. During the fatigue measurement, a standard signal with five pulses of identical pulse widths and magnitudes [20] was used, as shown in the inset of Fig. 6 (dashed line). The first pulse, P_s, presets the PVDF film to a given polarization state. The second pulse switches the PVDF film to the opposite state and measures the switched polarization. The measurement of the two pulses at voltage contains remanent and non-remanent polarizations; P^* measures the remanent and non-remanent polarization and $\hat{P}$ measures only the non-remanent polarization.

The effects of fatigue on polarization switching kinetics are shown in Fig. 6. The duration test had one million cycles with a frequency of 1 kHz and a voltage of 9 V. The suppression of duration polarization for all characterized fatigues reaches a constant value of about 3.05 nC/cm^2. However, the PVDF film induced larger degradation when the number of stress cycles was increased to about 105 cumulative cycles. The fatigue degradation of PVDF film is attributed to an increase of the activation field for dipole switching and a suppression of switching polarization [2].

4. CONCLUSION

The crystallization, frequency responses, hysteresis, leakage currents, I-V characteristics, and fatigue characteristics of PVDF film were investigated for flexible electronics applications. The I-V characteristics of PVDF film exhibit Schottky-like behavior. The maximum leakage currents of PVDF film with DC bias voltages is 3.46 pA for an input voltage of 9 V. The maximum polarizations for applied voltages of 1, 5, and 10 V are 0.37, 1.531, and 3.07 pF/cm^2, respectively. The characterized fatigue of PVDF film reaches

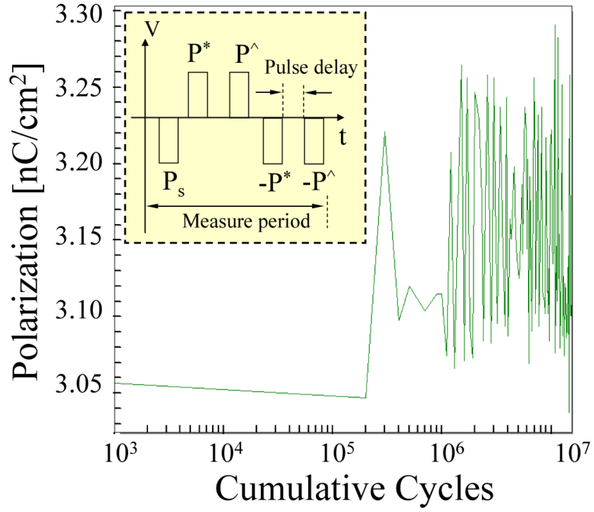

Fig. 6. Effects of fatigue on polarization switching at one million cycles obtained at a frequency of 1 kHz and a voltage of 9 V.

a constant value of about 3.05 nC/cm^2. An increase in leakage current is caused by electrically conductive channels spreading out within the PVDF due to material breakdown. The hysteretic behavior of PVDF is due to the loss nature of the piezoelectric material. The resistive load exhibits high-pass filter characteristics. The electriomechanical results show that PVDF can be applied to flexible electronics.

ACKNOWLEDGEMENT

This work was supported by the National Science Council of Taiwan (under grant NSC 102-2221-E-150-014), Common Laboratories for Micro/Nano Science and Technology of National Formosa University.

REFERENCES

1. Mao, D., Mejia, I., Stiegler, H., Gnade, B.E. and Quevedo-Lopez, M.A., "Fatigue characteristics of poly(vinylidene fluoride-trifluoroethylene) copolymer ferroelectric thin film capacitors for flexible electronics memory applications", *Organic Electronics*, Vol. 12, No. 8, pp. 1298–1303, 2011.
2. Chang, W.Y., Lin, Y.C. and Chu, C.H., "A flexible piezoelectric sensor for microfluidic applications using polyvinylidene fluoride", *IEEE Sensors Journal*, Vol. 8, No. 5, pp. 495–500, 2008.
3. Zhou, J., Fei, P., Gu, Y., Mai, W., Gao, Y., Yang, R., Bao, G. and Wang, Z.L., "Piezoelectric-potential-controlled polarity-reversible Schottky diodes and switches of ZnO wires", *Nano Letters*, Vol. 8, No. 11, pp. 3973–3977, 2008.
4. Wang, Z.L., "Piezotronic and piezophototronic effects", *The Journal of Physical Chemistry Letters*, Vol. 1, No. 9, pp. 1388–1393, 2010.
5. Kim, H.J., Lee, C.H., Kim, D.W. and Yi, G.C., "Fabrication and electrical characteristics of dual-gate ZnO nanorod metal-oxide semiconductor field-effect transistors", *Nanotechnology*, Vol. 17, No. 11, pp. S327–S331, 2006.
6. Galoppini, E., Rochford,J., Chen, H., Saraf, G., Lu, Y., Hagfeldt, A. and Boschloo, G., "Fast electron transport in metal organic vapor deposition grown dye-sensitized ZnO nanorod solar cells", *The Journal of Physical Chemistry B*, Vol. 110, No. 33, pp. 16159–16161, 2006.
7. Baxter, J.B., Walker, A.M., van Ommering, K. and Aydil, E.S., "Synthesis and characterization of ZnO nanowires and their integration into dye-sensitized solar cells", *Nanotechnology*, Vol. 17, No. 11, pp. S304, 2006.
8. Chang, W.Y., Fang, T.H. and Lin, Y.C., "Physical characteristics of polyimide films for flexible sensors", *Applied Physics A*, Vol. 92, pp. 693–701, 2008.

9. Chang, W.Y., Fang, T.H., Weng, C.I. and Yang, S.S., "Flexible piezoelectric harvesting based on epitaxial growth of ZnO", *Applied Physics A*, Vol. 102, No. 3, pp. 705–711, 2011.
10. Khan, M.A., Bhansali, U. and Alshareef, H.N., "All-polymer, transparent and flexible ferroelectric memory device", *Organic Electronics*, Vol. 12, p. 2225, 2011.
11. Sun, L.L., Li, B., Zhang, Z.G. and Zhong, W.H., "Achieving very high fraction of beta-crystal PVDF and PVDF/CNF composites and their effect on AC conductivity and microstructure through a stretching process", *European Polymer Journal*, Vol. 46, No. 11, pp. 2112–2119, 2010.
12. Chang, W.Y., Fang, T.H., Liu, S.Y. and Lin, Y.C., "Phase transformation and thermomechanical characteristics of stretched polyvinylidene fluoride", *Materials Science and Engineering A*, Vol. 8, Nos. 1–2, pp. 477–482, 2008.
13. Mohajir, B.E. and Heymans, N., "Changes in structural and mechanical behaviour of PVDF with processing and thermomechanical treatments", *Polymer*, Vol. 42, No. 13, pp. 5661–5667, 2001.
14. Chang, W.Y., Fang, T.H. and Lin, Y.C., "Thermomechanical and optical characteristics of stretched polyvinylidene fluoride", *Journal of Polymer Science: Part B: Polymer Physics*, Vol. 46, No. 10, pp. 949–958, 2008.
15. Mano, J.F., Sencadas, V., Costa, A.M. and Mendez, S.L., "Dynamic mechanical analysis and creep behaviour of "β-PVDF films", *Materials Science and Engineering: A*, Vol. 370, Nos. 1–2, pp. 336–340, 2004.
16. Vinogradov, A.M. and Holloway, F., "Dynamic mechanical testing of the creep and relaxation properties of polyvinylidene fluoride", *Polymer Test*, Vol. 19, No. 2, pp. 131–142, 2000.
17. Lee, H. and Bhushan, B., "Nanotribology of polyvinylidene difluoride (PVDF) in the presence of electric field", *Journal of Colloid and Interface Science*, Vol. 360, No. 2, pp. 777–784, 2011.
18. Smith, R.C. and Hom, C.L., "A domain wall theory for ferroelectric hysteresis", *Journal of Intelligent Material Systems and Structures*, Vol. 10, No. 2, pp. 195–213, 1999.
19. Scheipl, G., Zirkl, M., Stadlober, B., Groten, J., Jakopic, G., Krenn, J.R., Sawatdee, A., Bodo, P. and Andersson, P., "Fabrication, characterization and modeling of PVDF based organic IR-sensors for human body recognition", *Inst. of Nanostructured Mater. & Photonics, IEEE Sensors*, pp. 1252–1255, 2009.
20. *RT66B Vision Ferroelectric Memory Characterization Manual*, Radiant Technologies, n.d.